Evaluating the Robustness of Text-to-image Diffusion Models against Real-world Attacks

Anonymous ACL submission

Abstract

Text-to-image (T2I) diffusion models (DMs) have shown promise in generating high-quality images from textual descriptions. The real-world applications of these models require particular attention to their safety and fidelity, which yet has not been sufficiently explored. One fundamental question is whether the existing T2I DMs are robust against variations over input texts. To answer it, this work provides the first robustness evaluation of T2I DMs against *real-world* perturbations. Unlike malicious attacks that involve apocryphal alterations to the input texts, we consider a perturbation space spanned by realistic errors (e.g., typo, glyph, phonetic) that humans can make and develop adversarial attacks to generate worst-case perturbations for robustness evaluation. Given the inherent randomness of the generation process, we design four novel distribution-based objectives to mislead T2I DMs. We optimize the objectives in a black-box manner without any knowledge of the model. Extensive experiments demonstrate the effectiveness of our method for attacking popular T2I DMs and simultaneously reveal their non-trivial robustness issues. Besides, we also offer an in-depth analysis to show our method is not specialized for solely attacking the text encoder in T2I DMs.

1 Introduction

Diffusion models (DMs) (Sohl-Dickstein et al., 2015; Ho et al., 2020) have demonstrated remarkable success in generating images and shown promise in diverse applications, including super-resolution (Saharia et al., 2022b), image inpainting (Lugmayr et al., 2022), text-to-image synthesis (Rombach et al., 2022; Ramesh et al., 2022), image editing (Brooks et al., 2022), video generation (Ho et al., 2022a,b; Yang et al., 2024), etc. A typical DM employs a forward process that gradually diffuses the data distribution towards a noise distribution and a reverse process that recovers the data through step-by-step denoising. Among the applications, text-to-image (T2I) generation has received significant attention and witnessed the development of large models such as GLIDE (Nichol et al., 2022), Imagen (Saharia et al., 2022a), DALL-E 2 (Ramesh et al., 2022), Stable Diffusion (Rombach et al., 2022), VQ-Diffusion (Gu et al., 2022), etc. These models typically proceed by conditioning the reverse process on the embeddings of textual descriptions obtained from certain text encoders. Their ability to generate high-quality images from textual descriptions can significantly simplify creation of game scenarios, book illustrations, organization logos, and more.

The robustness of T2I DMs against perturbations to the input text plays a vital role in ensuring their reliability in practical use. Initial studies investigating this have shown that T2I DMs can be vulnerable to adversarial attacks (Du et al., 2023; Yang et al., 2023; Zhang et al., 2024)—by applying subtle perturbations to the input text, the generated image deviates significantly from the intended target. However, these works primarily focus on malicious attacks, e.g., creating meaningless or distorted custom words (Millière, 2022) or phrases (Maus et al., 2023), adding irrelevant distractions (Zhuang et al., 2023), etc., which often introduce substantial changes to the text and may rarely occur in real-world scenarios. We shift our attention from intentional attacks to everyday errors such as typos, grammar mistakes, or vague expressions, as suggested by related work in natural language processing (Li et al., 2018; Eger and Benz, 2020; Eger et al., 2019a; Le et al., 2022), to thoroughly evaluate the robustness of models that interact with humans in **practical** use. It is of particular importance to evaluate and understand the robustness of T2I DMs since a more robust model can enhance user efficiency by avoiding the need to go back and check mistakes in the prompts and make corrections after generating erroneous images.

A giant ice cream sculpture towering over a miniature town. | A giant ice creeam sculpture towering over a miniature town. | A giant ice cream sculpture towering over a miniature town. | A giant icae cream sculpture towering over a miniature town.

Figure 1: An illustration of our attack method against Stable Diffusion (Rombach et al., 2022) based on three attack rules (detailed in Section 2.3.1). Adversarially modified content is highlighted in red. Note that the red 'e' (U+0435) in Glyph is different from 'e' (U+0065) in the original sentence.

This work provides the first evaluation of the robustness of T2I DMs against *real-world* perturbations. As discussed, we consider an attack space spanned by realistic errors that humans can make to ensure semantic consistency, including typos, glyphs, and phonetics. To tackle the inherent uncertainty in the generation process of DMs, we develop novel distribution-based attack objectives to mislead T2I DMs. We perform attacks in a black-box manner using greedy search to avoid assumptions about the model. Technically, our attack algorithm first identifies the keywords based on the words' marginal influence on the generation distribution and then applies elaborate character-level replacements. Our algorithm can be used by the model developers to evaluate the robustness of their T2I DMs before being deployed in the wild.

We perform extensive empirical evaluations on datasets of artificial prompts and image captions. We first conduct a set of diagnostic experiments to prioritize the different variants originated from the distribution-oriented attack objectives, which also reflects the vulnerability of existing T2I DMs. We then provide an interesting discussion on the target of attacking DMs: the text encoder only vs. the whole diffusion process. Finally, we attack T2I DMs (SD v2.1 and SDXL) in real-world settings and observe high success rates, even in the case that the perturbation rates and query times are low. Additionally, we also give a qualitative case study on a closed-source generative model, DALL-E 2.

2 Methodology

This section provides a detailed description of our approach to real-world adversarial attacks of T2I DMs. We briefly outline the problem formulation before delving into the design of attack objective functions and then describe how to perform optimization in a black-box manner. Figure 2 displays the overview of our method.

2.1 Problem Formulation

A T2I DM that accepts a text input c and generates an image x essentially characterizes the conditional distribution $p_\theta(x|c)$ with θ as model parameters. To evaluate the robustness of modern DMs so as to govern their behaviors when adopted in the wild, we opt to attack the input text, i.e., finding a text c' which keeps close to the original text c but can lead to a significantly biased generated distribution. Such an attack is meaningful in the sense of encompassing real-world perturbations such as typos, glyphs, and phonetics. Concretely, the optimization problem is formulated as:

$$\max_{c'} \mathcal{D}(p_\theta(x|c') \| p_\theta(x|c)), \quad \text{s.t. } d(c, c') \leq \epsilon, \tag{1}$$

where $\mathcal{D}$ denotes a divergence measure between two distributions, $d(c, c')$ measures the the text distance, and ϵ indicates the perturbation budget.

The main challenge of attack lies in that we cannot write down the exact formulation of $p_\theta(x|c)$ and $p_\theta(x|c')$ of DMs but get only a few i.i.d. samples $\{\bar{x}_1, \ldots, \bar{x}_N\}$ and $\{x_1, \ldots, x_N\}$ from them, where $\bar{x}_i$ is an image generated with original text c while x_i is generated with modified text c'.

2.2 Attack Objectives

We develop four instantiations of the distribution-based attack objective, as defined in Eq. (1).

2.2.1 MMD Distance

As validated by the community (Dziugaite et al., 2015; Tolstikhin et al., 2016), the maximum mean discrepancy (MMD) is a widely used metric to distinguish two distributions given finite samples. Formally, assuming access to a kernel function κ, the square of MMD distance is typically defined as:

$$\mathcal{D}_{\text{MMD}^2}\big(p_\theta(x \mid c') \| p_\theta(x \mid c)\big) \approx \frac{1}{N^2}\sum_{i=1}^{N}\sum_{j=1}^{N}\kappa(x_i, x_j) - \frac{2}{N^2}\sum_{i=1}^{N}\sum_{j=1}^{N}\kappa(x_i, \bar{x}_j) + C, \tag{2}$$

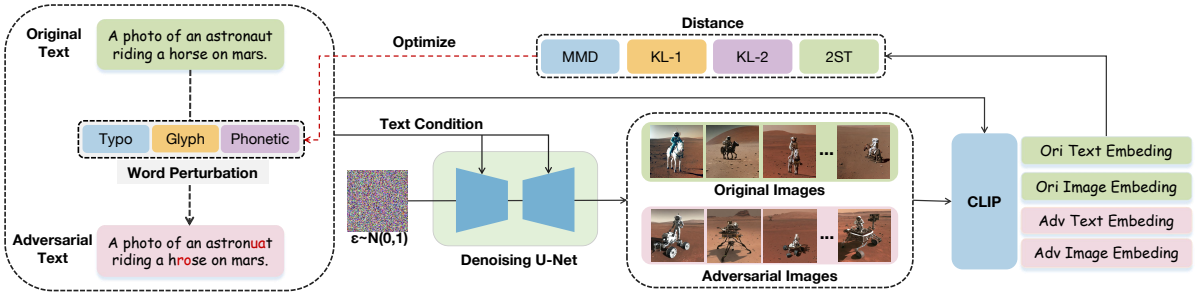

Figure 2: An illustration of our attack pipeline for evaluating the robustness of T2I DMs.

where C refers to a constant agnostic to c'. The feature maps associated with the kernel should be able to help construct useful statistics of the sample set such that MMD can compare distributions. In the case that x is an image, a valid choice is a deep kernel built upon a pre-trained NN-based image encoder h (e.g., a ViT trained by the objective of MAE (He et al., 2022) or CLIP (Radford et al., 2021)). In practice, we specify the kernel with a simple cosine form $\kappa(x, x') := h(x)^\top h(x')/\|h(x)\|\|h(x')\|$ given that h's outputs usually locate in a well-suited Euclidean space.

2.2.2 KL Divergence

Considering that text also provides crucial information in the attack process, we will incorporate text information to consider the joint distribution of images and texts. Due to the excellent ability of CLIP to represent both image and text information while preserving their relationships, we have chosen to use CLIP as the model for encoding images and texts. Assume access to a pre-trained ϕ-parameterized CLIP model comprised of an image encoder h_ϕ and a text encoder g_ϕ and assume the output features to be L^2-normalized. It can provide a third-party characterization of the joint distribution between the image x and the text c for guiding attack. Note that $h_\phi(x)^\top g_\phi(c)$ measures the likelihood of the coexistence of image x and text c, thus from a probabilistic viewpoint, we can think of $e_\phi(x, c) := \alpha h_\phi(x)^\top g_\phi(c)$, where α is some constant scaling factor, as $\log p_\phi(x, c)$. Under the mild assumption that $p_\phi(x|c)$ approximates $p_\theta(x|c)$, we instantiate the measure $\mathcal{D}$ in Eq. (1) with KL divergence and derive the following maximization objective (details are deferred to Appendix C).

$$\begin{aligned}&\mathcal{D}_{\mathrm{KL}}\big(p_\theta(x \mid c')\|p_\theta(x \mid c)\big)\\&\approx \mathbb{E}_{p_\theta(x|c')}\big[-e_\phi(x,c)\big] + \mathbb{E}_{p_\theta(x|c')}\big[\log p_\theta(x \mid c')\big] + C\end{aligned} \tag{3}$$

where C denotes a constant agnostic to c'. The first term corresponds to generating images containing semantics contradictory to text c and can be easily computed by Monte Carlo (MC) estimation. The second term is negative entropy, so the maximization of it means reducing generation diversity. Whereas, in practice, the entropy of distribution over high-dimensional images cannot be trivially estimated given a few samples. To address this issue, we replace $\mathbb{E}_{p_\theta(x|c')}[\log p_\theta(x|c')]$ with a lower bound $\mathbb{E}_{p_\theta(x|c')}[\log q(x)]$ for any probability distribution q, due to that $\mathcal{D}_{\mathrm{KL}}(p_\theta(x|c')\|q(x)) = \mathbb{E}_{p_\theta(x|c')}[\log p_\theta(x|c') - \log q(x)] \geq 0$. In practice, we can only acquire distributions associated with the CLIP model, so we primarily explore the following two strategies.

Strategy 1 (KL-1). $\log q(x) := \log p_\phi(x, c') = e_\phi(x, c')$. Combining with Eq. (3), we obtain (C is omitted):

$$\begin{aligned}&\mathcal{D}_{\mathrm{KL}}(p_\theta(x|c')\|p_\phi(x|c)) \geq \mathbb{E}_{p_\theta(x|c')}[e_\phi(x,c') - e_\phi(x,c)]\\&\approx \alpha\Big[\frac{1}{N}\sum_{i=1}^{N} h_\phi(x_i)\Big]^\top \Big(g_\phi(c') - g_\phi(c)\Big).\end{aligned} \tag{4}$$

The adversarial text c' would affect both the generated images x_i and the text embeddings $g_\phi(c')$. Therefore, it is likely that by maximizing the resulting term in Eq. (4) w.r.t. c', the text encoder of the CLIP model is attacked (i.e., $g_\phi(c') - g_\phi(c)$ is pushed to align with the average image embedding), which deviates from our goal of delivering a biased generation distribution.

Strategy 2 (KL-2). $\log q(x) := \log p_\phi(x) = \mathrm{L}_{\hat{c}\in\mathcal{C}}(e_\phi(x, \hat{c})) - \log|\mathcal{C}|$ where L is the log-sum-exp operator and $\mathcal{C}$ denotes the set of all possible text inputs. Likewise, there is (we omit constants):

$$\begin{aligned}&\mathcal{D}_{\mathrm{KL}}(p_\theta(x|c')\|p_\phi(x|c)) \geq \mathbb{E}_{p_\theta(x|c')}[\mathrm{L}_{\hat{c}\in\mathcal{C}}(e_\phi(x,\hat{c})) - e_\phi(x,c)]\\&\approx \frac{1}{N}\sum_{i=1}^{N}\big[\mathrm{L}_{\hat{c}\in\mathcal{C}}(e_\phi(x_i,\hat{c})) - e_\phi(x_i,c)\big].\end{aligned} \tag{5}$$

As shown, the first term pushes the generated images toward the high-energy regions, and the second hinders the generated images from containing

semantics about c. To reduce the computational overhead, we draw a set of commonly used texts and pre-compute their text embeddings via CLIP before attacking. Then, during attacking, we only need to send the embeddings of generated images to a linear transformation followed by an L operator to get an estimation of the first term of Eq. (5).

2.2.3 Two-sample Test

In essence, distinguishing $p_\theta(x|c')$ and $p_\theta(x|c)$ by finite observations corresponds to a two-sample test (2ST) in statistics, and the aforementioned MMD distance is a test statistic that gains particular attention in the machine learning community. Based on this point, we are then interested in building a general framework that can embrace existing off-the-shelf two-sample test tools for attacking T2I DMs. This can considerably enrich the modeling space. Basically, we define a unified test statistic in the following formula:

$$\hat{t}\Big(\{\varphi(x_i)\}_{i=1}^N, \{\varphi(\bar{x}_i)\}_{i=1}^N\Big). \tag{6}$$

Roughly speaking, we will reject the null hypothesis $p_\theta(x|c') = p_\theta(x|c)$ when the statistic is large to a certain extent. The function $\hat{t}$ in the above equation is customized by off-the-shelf two-sample test tools such as KS test, t-test, etc. Considering the behavior of these tools may quickly deteriorate as the dimension increases (Gretton et al., 2012), we introduce a projector φ to produce one-dimensional representations of images x. As a result, φ implicitly determines the direction of our attack. For example, if we define φ as a measurement of image quality in terms of FID (Heusel et al., 2017), then by maximizing Eq. (6), we will discover c' that leads to generations of low quality. Recalling that our original goal is a distribution of high-quality images deviated from $p_\theta(x|c)$, we hence want to set $\varphi(\cdot) := \log p_\theta(\cdot|c)$, which, yet, is inaccessible. Reusing the assumption that the conditional distribution captured by a CLIP model can form a reasonable approximation to $p_\theta(x|c)$, we set $\varphi(\cdot)$ to the aforementioned energy score $e_\phi(\cdot, c)$, which leads to the following test statistic:

$$\mathcal{D}_{\text{2ST}}(p_\theta(x|c')\|p_\theta(x|c)) := \hat{t}\Big(\{e_\phi(x_i, c)\}_{i=1}^N, \{e_\phi(\bar{x}_i, c)\}_{i=1}^N\Big). \tag{7}$$

We empirically found that the t-test tool can yield a higher attack success rate compared to other two-sample test tools, hence we use the t-test tool as the default option in the following.

2.3 Attack Method

Based on the attack objectives specified above, here we establish a real-world-oriented word search space and implement a greedy search strategy to find adversarial input text for T2I DMs.

2.3.1 Perturbation Rules

Following recent related works (Eger and Benz, 2020; Eger et al., 2019a; Le et al., 2022; Chen et al., 2022, 2023), we include the following three kinds of perturbations into the search space of our attack algorithm: (1) **Typo** (Li et al., 2018; Eger and Benz, 2020), which comprises seven fundamental operations for introducing typos into the text, including randomly deleting, inserting, replacing, swapping, adding space, transforming case, and repeating a single character; (2) **Glyph** (Li et al., 2018; Eger et al., 2019a), which involves replacing characters with visually similar ones; (3) **Phonetic** (Le et al., 2022), which involves replacing characters in a way that makes the whole word sound similar to the original one. We present examples of these three perturbation rules in Appendix B.

2.3.2 Greedy Search

Given the efficiency and effectiveness of greedy algorithms in previous black-box text attack problems (Feng et al., 2018; Pruthi et al., 2019), we also employ greedy algorithm here and organize it as the following steps.

Step 1: word importance ranking. Given a sentence of n words $c = \{w_1, w_2, ..., w_n\}$, it is usually the case that only some keywords act as the influential factors for controlling DMs. Therefore, we aim to first identify such words and then perform attack. The identification of word importance is trivial in a white-box scenario, e.g., by inspecting model gradients (Behjati et al., 2019), but is challenging in the considered black-box setting. To address this, we directly measure the marginal influence of the word w_i on the generation distribution via $I_{w_i} := \mathcal{D}(p_\theta(x|c\backslash w_i)\|p_\theta(x|c))$ where $c\backslash w_i = \{w_1, ..., w_{i-1}, w_{i+1}, ...w_n\}$ denotes the sentence without the word w_i and $\mathcal{D}$ refers to the divergence measure defined earlier. With this, we can compute the influence score I_{w_i} for each word w_i in the sentence c, and then obtain a ranking over the words according to their importance.

Step2: word perturbation. We then perturb the detected important words to find the adversarial example c'. For the most important word $w_i \in c$,

we randomly select one character in it and then randomly apply one of the meta-operations in the perturbation rule of concern, e.g., character swapping and deleting, to obtain a perturbed word as well as a perturbed sentence. Repeating this five times results in 5 perturbed sentences $\{c'_1, c'_2, ...c'_5\}$. We select the sentence leading to the highest generation divergence from the original sentence, i.e., $\mathcal{D}(p_\theta(x|c'_i)\|p_\theta(x|c)), \forall i \in \{1, \ldots, 5\}$ as the adversarial sentence c'. If the attack has not reached the termination condition, the next word in the importance ranking will be selected for perturbation.

3 Diagnostic Experiments

In this section, we provide diagnostic experiments consisting of two aspects: (1) assessing the four proposed attack objectives under varying perturbation rates; (2) analyzing which part of the DM is significantly misled. These analyses not only validate the efficacy of our method, but also deepen our understanding of the robustness of T2I DMs, and provide insightful perspectives for future works.

Datasets. We consider two types of textual data for T2I generation: (1) 50 ChatGPT generated (ChatGPT-GP) prompts by querying: "generate 50 basic prompts used for image synthesis." and (2) 50 captions from SBU Corpus (Ordonez et al., 2011). Such a dataset facilitates a thorough investigation of the efficacy and applicability of our method in practical image-text generation tasks.

Victim Models. We choose Stable Diffusion (SD) v2.1 (Rombach et al., 2022) as the victim model due to its widespread usage, availability as an open-source model, and strong generation capability. Stable Diffusion utilizes a denoising mechanism that operates in the latent space of images and incorporates cross-attention to leverage guidance information. Text inputs are first processed by CLIP's text encoder to generate text embeddings, which are subsequently fed into the cross-attention layers to aid in image generation.

Evaluation Metrics. We use the CLIP Score (Hessel et al., 2021), esentially the aforementioned $h_\phi(x)^\top g_\phi(c)$, to measure the semantic similarity between the original text c and the generated images $\{x_1, \ldots, x_N\}$ based on the adversarial text c'. Specifically, we define the metric $S_{I2T} = \frac{1}{N}\sum_{i=1}^{N} \max(0, 100 \cdot g_\phi(c)^\top h_\phi(x'))$ over the generated images, and we hypothesize that a higher S_{I2T} indicates a less adversarial text c'. Typically, N is set to 15 to balance efficiency and fidelity. We can also calculate the similarity between the original text c and the adversarial text c' with $S_{T2T} = \max(0, 100 \cdot g_\phi(c)^\top g_\phi(c'))$. Though these two metrics use the same notations as our attack objectives, we actually use various pre-trained CLIPs to instantiate them to avoid over-fitting—employing the CLIP with VIT-L-patch14 backbone for attacking while using VIT-L-patch14-336 backbone for evaluation.

3.1 Attack with Different Objectives

We conduct diagnostic experiments on the four attack objectives under various perturbation rules. The perturbation rate is defined as the ratio of perturbed words to total words, varying from 0% to 100% with 10% intervals. Figure 3 reports the average S_{I2T} on ChatGPT-GP and SBU Corpus, with a random baseline for comparison.

On ChatGPT-GP, all methods exhibit a declining trend in S_{I2T} as the perturbation rate increases. Considering high perturbation rates rarely exist in practice, we primarily focus on situations where the perturbation rate below 50%. Within this range, the curves corresponding to MMD, KL-2, and 2ST display a rapid decrease across all three perturbation rules, more than $2\times$ faster than random and KL-1 when using typo and glyph rules. It is also noteworthy that MMD and 2ST perform similarly and yield the best overall results.

On SBU Corpus, 2ST is evidently more effective than MMD. Additionally, even with a perturbation rate of 100%, the random method fails to achieve a similar S_{I2T} score compared to other methods. This observation suggests the effectiveness of our attack algorithm. Additionally, glyph-based perturbations lead to the most rapid performance drop, followed by typo perturbations, and phonetic perturbations lead to the slowest drop. This disparity may be attributed to glyph perturbations completely disrupting the original word embedding.

3.2 Analysis of Misled Components

Previous studies suggest that attacking only the CLIP encoder is sufficient for misleading diffusion models (Zhuang et al., 2023). However, our method is designed to attack the entire generation process instead of the CLIP encoder. For empirical evaluation, we conduct experiments in this section.

We include two additional attack methods: attacking only the CLIP encoder and attacking only the diffusion process. Regarding this first one, we focus solely on maximizing the dissimilarity between the original text and the adversarial one.

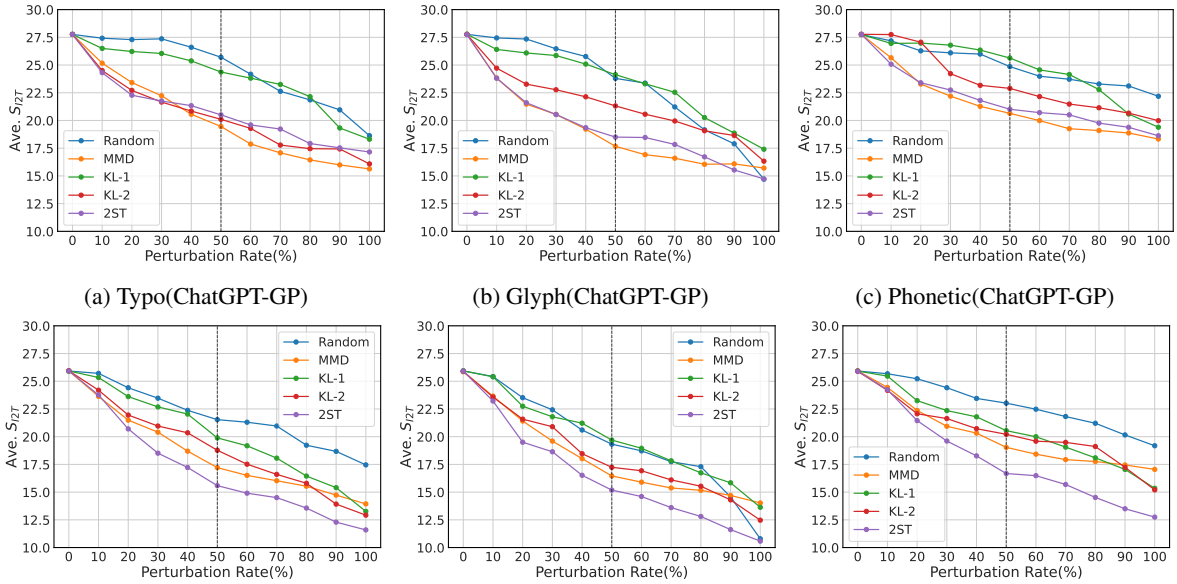

(a) Typo(ChatGPT-GP) (b) Glyph(ChatGPT-GP) (c) Phonetic(ChatGPT-GP)

(d) Typo(SBU Corpus) (e) Glyph(SBU Corpus) (f) Phonetic(SBU Corpus)

Figure 3: CLIP Score at different perturbation rates on ChatGPT-GP and SBU Corpus. The perturbation rate is the ratio between the number of perturbed words and the total words in a sentence

To achieve this, we employ S_{T2T} as the optimization objective, i.e., $\mathcal{D}_{\text{CLIP}} = S_{T2T} = \max(0, 100 \cdot g_\phi(c)^\top g_\phi(c'))$. As for the second one, we modify Eq. (4) and devise a new attack objective as follows (α and β denote two trade-off coefficients):

$$\mathcal{D}_{\text{DP}} \approx \left[\alpha g_\phi(c') - \beta \frac{1}{N} \sum_{i=1}^{N} h_\phi(x_i)\right]^\top g_\phi(c). \quad (8)$$

While maximizing the distance between the original text and the adversarial images, we also aim to ensure that the representations of the adversarial text and the original text are as similar as possible. This confines that even though the entire DM is under attack, the CLIP encoder remains safe.

In the following, we demonstrate why Eq. (8) represents only the attack diffusion process here. For Eq. (8), we can expand it as:

$$\begin{aligned}\mathcal{D}_{\text{DP}} &\approx \left[\alpha g_\phi(c') - \beta \frac{1}{N} \sum_{i=1}^{N} h_\phi(x_i)\right]^\top g_\phi(c) \\ &= \alpha g_\phi(c')^\top g_\phi(c) - \beta \left[\frac{1}{N} \sum_{i=1}^{N} h_\phi(x_i)\right]^\top g_\phi(c)\end{aligned} \quad (9)$$

where c is the original text, c' is the modified text generating x_i. The first term, $\alpha g_\phi(c')^\top g_\phi(c)$, measures the similarity between the original text and the adversarial text. The second term, $\beta \left[\frac{1}{N} \sum_{i=1}^{N} h_\phi(x_i)\right]^\top g_\phi(c)$, represents the similarity between the original text and the adversarially generated images. Maximizing this objective constrains the original text and the adversarial text to be as similar as possible after being encoded by the text encoder, while minimizing the similarity between the original text and the adversarial generated images. In this way, it avoids attacking the text encoder and solely attacks the diffusion process.

Since Eq. (8) is modified from Eq. (4), we also provide an expanded explanation for Eq. (4) as:

$$\begin{aligned}\mathcal{D}_{\text{KL}}(p_\theta(x|c') \| p_\phi(x|c)) &\approx \alpha \left[\frac{1}{N} \sum_{i=1}^{N} h_\phi(x_i)\right]^\top \left(g_\phi(c') - g_\phi(c)\right) \\ &= \alpha \left[\frac{1}{N} \sum_{i=1}^{N} h_\phi(x_i)\right]^\top g_\phi(c') - \alpha \left[\frac{1}{N} \sum_{i=1}^{N} h_\phi(x_i)\right]^\top g_\phi(c)\end{aligned} \quad (10)$$

The first term, $\alpha \left[\frac{1}{N} \sum_{i=1}^{N} h_\phi(x_i)\right]^\top g_\phi(c')$, measures the similarity between the adversarial text and adversarially generated images. The second term, $\alpha \left[\frac{1}{N} \sum_{i=1}^{N} h_\phi(x_i)\right]^\top g_\phi(c)$, represents the similarity between the original text and the adversarial generated images. Maximizing this objective constrains the encoded adversarial text and the adversarial images to be as similar as possible, which essentially ensures the quality of the text embedding guided image diffusion process, while minimizing the similarity between the original text and the adversarial generated images. In this way, it avoids attacking the diffusion process and solely attacks the text encoder, different from Eq. (8).

Given the poor performance of the random and KL-1 methods, we exclude them from this study. Considering that high perturbation rates are almost impossible in the real world, we experiment with perturbation rates only from 0% to 80%. We compute the average S_{I2T} and S_{T2T} across all texts at each rate, and plot their correlations in Figure 4.

As shown, exclusively targeting the CLIP en-

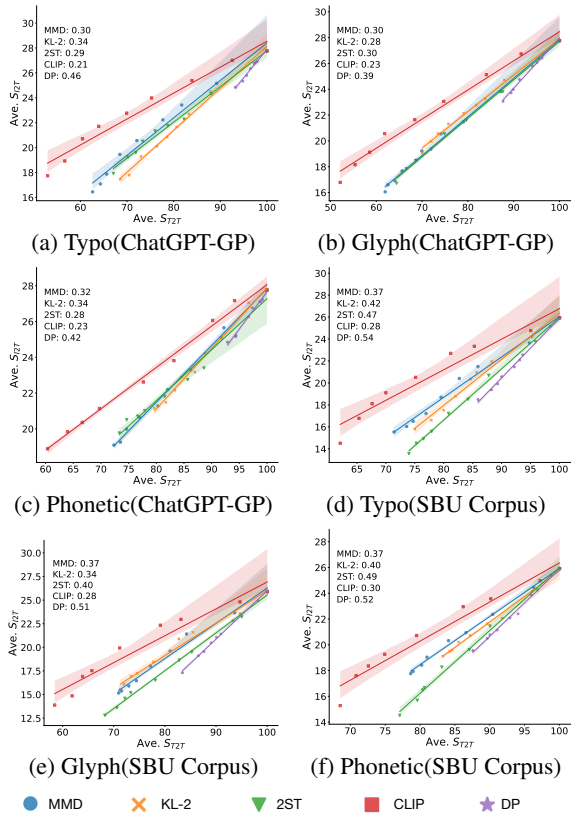

Figure 4: Corelation between S_{I2T} and S_{T2T} on ChatGPT-GP and SBU Corpus. The numbers in the upper-left corner represent the slopes of the lines.

coder yields the minimum regression slope, while solely attacking the diffusion process produces the maximum slope. For instance, on ChatGPT-GP with typo perturbations, the attack method solely attacking the CLIP encoder exhibits a slope of 0.21, whereas the attack method exclusively targeting the diffusion process shows a slope of 0.46. Attack methods that simultaneously target both processes display slopes between these extremes. These clearly support that our attack objectives simultaneously attack the CLIP encoder and the diffusion process. Furthermore, through the slope information, we can conclude that directly attacking the diffusion process yields a more significant decrease in image-text similarity at a given textual semantic divergence. Across all datasets and perturbation spaces, the slope disparity between direct attacks on the diffusion process and direct attacks on the CLIP encoder typically exceeds 0.1, with a maximum of 0.15.

3.3 Compare with Non-distribution Attack

We conduct a comparison experiment between our distribution-based optimization objective 2ST and a non-distribution method that minimizes the S_{I2T}

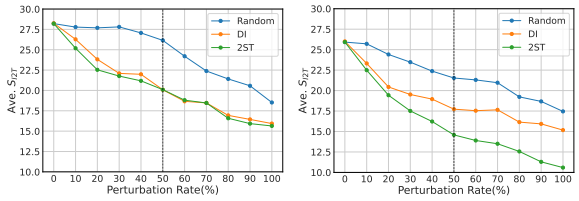

Figure 5: CLIP Score at different perturbation rates on ChatGPT-GP and SBU Corpus with typo rule.

of the prompt and a single definite image (DI). We randomly sampled 20 texts from ChatGPT-GP and SBU Corpus separately, then applied the typo rule to perturb sampled texts with different perturbation rates. The results, depicted in Figure 5, clearly demonstrate the superior effectiveness of our distribution-based approach.

4 Real-world Attack Experiment

Based on the preceding analysis, we identify that 2ST and MMD are two good attack objectives for T2I DMs. In this section, we will carry out attacks in real-world scenarios, where termination conditions are incorporated to balance the perturbation level and effectiveness.

Datasets. For a more comprehensive evaluation for our attack method in realistic scenarios, we incorporate two additional datasets. DiffusionDB (Wang et al., 2022b) contains 14 million T2I prompts, while LAION-COCO (Schuhmann et al., 2021) includes captions for 600 million images from LAION-5B (Schuhmann et al., 2022), generated via an ensemble of BLIP L/14 (Li et al., 2022) and two CLIP (Radford et al., 2021) variants. To conjoin diversity and efficiency, we randomly select 100 examples from each of the aforementioned datasets. Additionally, we also increased the size of ChatGPT-GP and SBU to 100 for this experiment.

Attack method. As said, we consider attacking based on MMD and 2ST. A threshold on the value of $\mathcal{D}$ is set for termination. If it is not reached, the attack terminates at a pre-fixed number of steps.

Evaluation metric. We use four metrics to evaluate our method in real-world attack scenes. (1) Levenshtein distance (L-distance), which measures the minimum number of single-character edits, a powerful indicator of the number of modifications made to a text. (2) Ori.S_{I2T} and Adv.S_{I2T} which indicate the similarity between the original text and original images as well as that between the original text and the adversarial images respectively. The mean and variance are both reported. (3) Average

Dataset	Attacker	Ori. S_{I2T}	Ave. Len.	L-distance	Adv. S_{I2T}	Ave. Query	Hum. Eval.
ChatGPT-GP	Typo	27.61±2.07	10.41	2.92	23.21±3.08	19.43	84.34%
	Glyph			2.27	23.09±2.75	18.63	84.65%
	Phonetic			5.38	22.67±3.58	17.78	86.16%
DiffusionDB	Typo	29.17±3.36	10.62	2.29	22.70±3.31	17.25	76.64%
	Glyph			1.81	22.71±3.22	16.30	76.64%
	Phonetic			5.04	22.91±3.34	16.27	75.51%
LAION-COCO	Typo	27.54±2.86	9.17	2.08	21.73±3.62	14.77	80.21%
	Glyph			1.85	21.32±3.69	15.11	81.89%
	Phonetic			5.04	21.76±3.87	16.15	79.32%
SBU Corpus	Typo	24.99±3.43	11.69	2.97	19.65±3.53	21.19	84.34%
	Glyph			2.42	19.01±3.76	20.54	85.41%
	Phonetic			5.85	18.86±3.91	19.92	85.41%

Table 1: Real-world attack with the **2ST** attack objective on SD v2.1.

Dataset	Attacker	Ori. S_{I2T}	Ave. Len.	L-distance	Adv. S_{I2T}	Ave. Query	Hum. Eval.
ChatGPT-GP	Typo	27.61±2.07	10.41	1.77	24.54±2.69	14.17	84.21%
	Glyph			1.15	24.88±2.67	13.08	84.36%
	Phonetic			3.81	26.08±2.21	14.58	80.02%
DiffusionDB	Typo	29.17±3.36	10.62	1.75	24.94±3.82	13.72	72.77%
	Glyph			1.29	24.81±3.90	13.41	73.53%
	Phonetic			4.27	26.71±3.24	15.13	70.09%
LAION-COCO	Typo	27.54±2.86	9.17	1.75	23.04±4.10	13.33	80.21%
	Glyph			1.35	23.72±3.91	12.35	82.04%
	Phonetic			3.62	25.06±3.09	13.21	77.37%
SBU Corpus	Typo	24.99±3.43	11.69	1.91	21.37±3.92	16.36	82.05%
	Glyph			1.37	21.44±3.66	15.01	82.33%
	Phonetic			3.72	23.15±3.25	16.20	79.67%

Table 2: Real-world attack with **MMD distance** attack objective on SD v2.1.

query times, which represents the number of times that DM generates images with one text, and serves as a metric for evaluating the attack efficiency. (4) Human evaluation, where humans are employed to assess the consistency between image and text. Each image-text pair are evaluated across three evaluators. Details are provided in Appendix D.

We first conduct the real-world attack experiment on **SD v2.1**. Table 1 and Table 2 present the results of real-attack experiments using various perturbation rules on different datasets, with 2ST and MMD objectives, respectively. Considering that our method involves querying each word of the sentence (described in Section 2.3.2), the query times minus the sentence length, which we named *true query times*, can better demonstrate the true efficiency of our approach. From this perspective, our method requires less than 10 *true query times* to achieve more than 4 S_{I2T} score drop across most datasets while maintaining > 75% *human evaluation* score. Simultaneously, we observe that our modifications are relatively minor. In the typo and glyph attacker, we require an *L-distance* of less than 3, while in the phonetic attacker, the threshold remains below 6. Furthermore, ChatGPT-GP and LAION-COCO are more susceptible to our attack, possibly attributed to their clearer and more flow sentence descriptions. In conclusion, with minimal modifications and limited queries to the model, we achieve a significant decrease in text-image similarity, substantiated by human evaluations.

Additional experiments and discussions are provided in the Appendices, including attacks on SDXL and DALL-E 2 (Appendix E.1 & E.3), complete comparisons with non-distribution attack (Appendix E.5), and analyses of defenses and manual attacks (Appendix E.4 & E.6). We also validate robustness of human evaluation in Appendix E.6.

5 Conclusion

In this work, we present a comprehensive evaluation of the robustness of DMs against real-world attacks. Unlike previous studies that focused on malicious alterations to input texts, we explore an attack method based on realistic errors that humans can make to ensure semantic consistency. Our novel distribution-based attack method can effectively mislead DMs in a black-box setting without any knowledge of the original generative model. Importantly, we show that our method does not solely target the text encoder in DMs, it can also attack the diffusion process. Even with extremely low perturbation rates and query times, our method can still achieve a high attack success rate.

Limitation

In our experiments, we employ DMs as the testbed and evaluate both random attack methods and our proposed method with four optimization objectives on our custom benchmark datasets. Due to limited resources, we focus on Stable Diffusion for the complete experiment and DALL-E 2 for the case study, given that our method involves 12 combinations of optimization objectives and perturbation rules. Therefore, conducting more comprehensive experiments covering different model architectures and training paradigms is a direction for future research.

Ethics Statement

A potential negative societal impact of our approach is that malicious attackers could exploit it to construct targeted attacks by modifying the loss function, leading to the generation of unhealthy or harmful images, thus causing security concerns. As more people focus on T2I DMs due to their excellent performance on image generation. In such scenarios, it becomes inevitable to address the vulnerability of DMs which can be easily attacked through black-box perturbation. Our work emphasizes the importance for developers of DMs to consider potential attacks that may exist in real-world settings during the training process.

References

Melika Behjati, Seyed-Mohsen Moosavi-Dezfooli, Mahdieh Soleymani Baghshah, and Pascal Frossard. 2019. Universal adversarial attacks on text classifiers. In *ICASSP 2019-2019 IEEE International Conference on Acoustics, Speech and Signal Processing (ICASSP)*, pages 7345–7349. IEEE.

Tim Brooks, Aleksander Holynski, and Alexei A Efros. 2022. Instructpix2pix: Learning to follow image editing instructions. *arXiv preprint arXiv:2211.09800*.

Daniel Cer, Yinfei Yang, Sheng-yi Kong, Nan Hua, Nicole Limtiaco, Rhomni St John, Noah Constant, Mario Guajardo-Cespedes, Steve Yuan, Chris Tar, and 1 others. 2018. Universal sentence encoder. *arXiv preprint arXiv:1803.11175*.

Yangyi Chen, Hongcheng Gao, Ganqu Cui, Fanchao Qi, Longtao Huang, Zhiyuan Liu, and Maosong Sun. 2022. Why should adversarial perturbations be imperceptible? rethink the research paradigm in adversarial NLP. In *Proceedings of the 2022 Conference on Empirical Methods in Natural Language Processing(EMNLP)*, pages 11222–11237. Association for Computational Linguistics.

Yangyi Chen, Hongcheng Gao, Ganqu Cui, Lifan Yuan, Dehan Kong, Hanlu Wu, Ning Shi, Bo Yuan, Longtao Huang, Hui Xue, and 1 others. 2023. From adversarial arms race to model-centric evaluation: Motivating a unified automatic robustness evaluation framework. *arXiv preprint arXiv:2305.18503*.

Ming Ding, Zhuoyi Yang, Wenyi Hong, Wendi Zheng, Chang Zhou, Da Yin, Junyang Lin, Xu Zou, Zhou Shao, Hongxia Yang, and 1 others. 2021. Cogview: Mastering text-to-image generation via transformers. *Advances in Neural Information Processing Systems*, 34:19822–19835.

Chengbin Du, Yanxi Li, Zhongwei Qiu, and Chang Xu. 2023. Stable diffusion is unstable. *ArXiv*, abs/2306.02583.

Gintare Karolina Dziugaite, Daniel M Roy, and Zoubin Ghahramani. 2015. Training generative neural networks via maximum mean discrepancy optimization. In *Proceedings of the Thirty-First Conference on Uncertainty in Artificial Intelligence*, pages 258–267.

Steffen Eger and Yannik Benz. 2020. From hero to zéroe: A benchmark of low-level adversarial attacks. In *Proc. of AACL*.

Steffen Eger, Gözde Gül Şahin, Andreas Rücklé, Ji-Ung Lee, Claudia Schulz, Mohsen Mesgar, Krishnkant Swarnkar, Edwin Simpson, and Iryna Gurevych. 2019a. Text processing like humans do: Visually attacking and shielding nlp systems. In *Proc. of NAACL*.

Steffen Eger, Gözde Gül Şahin, Andreas Rücklé, Ji-Ung Lee, Claudia Schulz, Mohsen Mesgar, Krishnkant Swarnkar, Edwin Simpson, and Iryna Gurevych. 2019b. Text processing like humans do: Visually attacking and shielding nlp systems. In *Proceedings of the 2019 Conference of the North American Chapter of the Association for Computational Linguistics: Human Language Technologies, Volume 1 (Long and Short Papers)*, pages 1634–1647.

Shi Feng, Eric Wallace, Alvin Grissom II, Mohit Iyyer, Pedro Rodriguez, and Jordan Boyd-Graber. 2018. Pathologies of neural models make interpretations difficult. In *Proceedings of the 2018 Conference on Empirical Methods in Natural Language Processing*, pages 3719–3728.

Brian Formento, Chuan-sheng Foo, Anh Tuan Luu, and See Kiong Ng. 2023. Using punctuation as an adversarial attack on deep learning-based nlp systems: An empirical study. In *Findings of the Association for Computational Linguistics: EACL 2023*, pages 1–34.

Oran Gafni, Adam Polyak, Oron Ashual, Shelly Sheynin, Devi Parikh, and Yaniv Taigman. 2022. Make-a-scene: Scene-based text-to-image generation with human priors. In *Computer Vision–ECCV 2022: 17th European Conference*, pages 89–106.

Arthur Gretton, Karsten M Borgwardt, Malte J Rasch, Bernhard Schölkopf, and Alexander Smola. 2012.

A kernel two-sample test. *The Journal of Machine Learning Research*, 13(1):723–773.

Shuyang Gu, Dong Chen, Jianmin Bao, Fang Wen, Bo Zhang, Dongdong Chen, Lu Yuan, and Baining Guo. 2022. Vector quantized diffusion model for text-to-image synthesis. In *IEEE/CVF Conference on Computer Vision and Pattern Recognition(CVPR)*, pages 10686–10696. IEEE.

Prakhar Gupta, Yulia Tsvetkov, and Jeffrey P Bigham. 2021. Synthesizing adversarial negative responses for robust response ranking and evaluation. In *Findings of the Association for Computational Linguistics: ACL-IJCNLP 2021*, pages 3867–3883.

Wenjuan Han, Liwen Zhang, Yong Jiang, and Kewei Tu. 2020. Adversarial attack and defense of structured prediction models. In *Proceedings of the 2020 Conference on Empirical Methods in Natural Language Processing (EMNLP)*, pages 2327–2338.

Kaiming He, Xinlei Chen, Saining Xie, Yanghao Li, Piotr Dollár, and Ross Girshick. 2022. Masked autoencoders are scalable vision learners. In *Proceedings of the IEEE/CVF Conference on Computer Vision and Pattern Recognition*, pages 16000–16009.

Xuanli He, Lingjuan Lyu, Lichao Sun, and Qiongkai Xu. 2021. Model extraction and adversarial transferability, your bert is vulnerable! In *Proceedings of the 2021 Conference of the North American Chapter of the Association for Computational Linguistics: Human Language Technologies*, pages 2006–2012.

Jack Hessel, Ari Holtzman, Maxwell Forbes, Ronan Le Bras, and Yejin Choi. 2021. Clipscore: A reference-free evaluation metric for image captioning. In *Proceedings of the 2021 Conference on Empirical Methods in Natural Language Processing*, pages 7514–7528.

Martin Heusel, Hubert Ramsauer, Thomas Unterthiner, Bernhard Nessler, and Sepp Hochreiter. 2017. Gans trained by a two time-scale update rule converge to a local nash equilibrium. *Advances in neural information processing systems*, 30.

Jonathan Ho, William Chan, Chitwan Saharia, Jay Whang, Ruiqi Gao, Alexey Gritsenko, Diederik P Kingma, Ben Poole, Mohammad Norouzi, David J Fleet, and 1 others. 2022a. Imagen video: High definition video generation with diffusion models. *arXiv preprint arXiv:2210.02303*.

Jonathan Ho, Ajay Jain, and Pieter Abbeel. 2020. Denoising diffusion probabilistic models. In *Advances in Neural Information Processing Systems*, volume 33, pages 6840–6851. Curran Associates, Inc.

Jonathan Ho, Tim Salimans, Alexey Gritsenko, William Chan, Mohammad Norouzi, and David J Fleet. 2022b. Video diffusion models. *arXiv preprint arXiv:2204.03458*.

Thai Le, Jooyoung Lee, Kevin Yen, Yifan Hu, and Dongwon Lee. 2022. Perturbations in the wild: Leveraging human-written text perturbations for realistic adversarial attack and defense. *arXiv preprint arXiv:2203.10346*.

Deokjae Lee, Seungyong Moon, Junhyeok Lee, and Hyun Oh Song. 2022. Query-efficient and scalable black-box adversarial attacks on discrete sequential data via bayesian optimization. In *International Conference on Machine Learning*, pages 12478–12497. PMLR.

Dianqi Li, Yizhe Zhang, Hao Peng, Liqun Chen, Chris Brockett, Ming-Ting Sun, and William B Dolan. 2021. Contextualized perturbation for textual adversarial attack. In *Proceedings of the 2021 Conference of the North American Chapter of the Association for Computational Linguistics: Human Language Technologies*, pages 5053–5069.

Jinfeng Li, Shouling Ji, Tianyu Du, Bo Li, and Ting Wang. 2018. Textbugger: Generating adversarial text against real-world applications. *arXiv preprint arXiv:1812.05271*.

Junnan Li, Dongxu Li, Caiming Xiong, and Steven Hoi. 2022. Blip: Bootstrapping language-image pre-training for unified vision-language understanding and generation. In *International Conference on Machine Learning*, pages 12888–12900. PMLR.

Linyang Li, Ruotian Ma, Qipeng Guo, Xiangyang Xue, and Xipeng Qiu. 2020. BERT-ATTACK: adversarial attack against BERT using BERT. In *Proceedings of the 2020 Conference on Empirical Methods in Natural Language Processing(EMNLP)*, pages 6193–6202.

Andreas Lugmayr, Martin Danelljan, Andres Romero, Fisher Yu, Radu Timofte, and Luc Van Gool. 2022. Repaint: Inpainting using denoising diffusion probabilistic models. In *Proceedings of the IEEE/CVF Conference on Computer Vision and Pattern Recognition*, pages 11461–11471.

Natalie Maus, Patrick Chao, Eric Wong, and Jacob Gardner. 2023. Adversarial prompting for black box foundation models. *arXiv preprint arXiv:2302.04237*.

Zhao Meng and Roger Wattenhofer. 2020. A geometry-inspired attack for generating natural language adversarial examples. In *Proceedings of the 28th International Conference on Computational Linguistics*, pages 6679–6689.

Raphaël Millière. 2022. Adversarial attacks on image generation with made-up words. *arXiv preprint arXiv:2208.04135*.

Alexander Quinn Nichol, Prafulla Dhariwal, Aditya Ramesh, Pranav Shyam, Pamela Mishkin, Bob Mcgrew, Ilya Sutskever, and Mark Chen. 2022. Glide: Towards photorealistic image generation and editing with text-guided diffusion models. In *International Conference on Machine Learning*, pages 16784–16804. PMLR.

Vicente Ordonez, Girish Kulkarni, and Tamara Berg. 2011. Im2text: Describing images using 1 million captioned photographs. In *Advances in Neural Information Processing Systems*, volume 24. Curran Associates, Inc.

Dustin Podell, Zion English, Kyle Lacey, Andreas Blattmann, Tim Dockhorn, Jonas Müller, Joe Penna, and Robin Rombach. 2023. Sdxl: Improving latent diffusion models for high-resolution image synthesis. *arXiv preprint arXiv:2307.01952*.

Danish Pruthi, Bhuwan Dhingra, and Zachary C Lipton. 2019. Combating adversarial misspellings with robust word recognition. In *Proceedings of the 57th Annual Meeting of the Association for Computational Linguistics*, pages 5582–5591.

Alec Radford, Jong Wook Kim, Chris Hallacy, Aditya Ramesh, Gabriel Goh, Sandhini Agarwal, Girish Sastry, Amanda Askell, Pamela Mishkin, Jack Clark, and 1 others. 2021. Learning transferable visual models from natural language supervision. In *International conference on machine learning*, pages 8748–8763. PMLR.

Aditya Ramesh, Prafulla Dhariwal, Alex Nichol, Casey Chu, and Mark Chen. 2022. Hierarchical text-conditional image generation with clip latents. *arXiv preprint arXiv:2204.06125*, 1(2):3.

Aditya Ramesh, Mikhail Pavlov, Gabriel Goh, Scott Gray, Chelsea Voss, Alec Radford, Mark Chen, and Ilya Sutskever. 2021. Zero-shot text-to-image generation. In *International Conference on Machine Learning*, pages 8821–8831.

Shuhuai Ren, Yihe Deng, Kun He, and Wanxiang Che. 2019. Generating natural language adversarial examples through probability weighted word saliency. In *Proceedings of the 57th Annual Meeting of the Association for Computational Linguistics*, pages 1085–1097.

Yuxi Ren, Xin Xia, Yanzuo Lu, Jiacheng Zhang, Jie Wu, Pan Xie, Xing Wang, and Xuefeng Xiao. 2024. Hyper-sd: Trajectory segmented consistency model for efficient image synthesis. *Preprint*, arXiv:2404.13686.

Robin Rombach, Andreas Blattmann, Dominik Lorenz, Patrick Esser, and Björn Ommer. 2022. High-resolution image synthesis with latent diffusion models. In *IEEE/CVF Conference on Computer Vision and Pattern Recognition(CVPR)*, pages 10674–10685. IEEE.

Chitwan Saharia, William Chan, Saurabh Saxena, Lala Li, Jay Whang, Emily L Denton, Kamyar Ghasemipour, Raphael Gontijo Lopes, Burcu Karagol Ayan, Tim Salimans, and 1 others. 2022a. Photorealistic text-to-image diffusion models with deep language understanding. *Advances in Neural Information Processing Systems*, 35:36479–36494.

Chitwan Saharia, Jonathan Ho, William Chan, Tim Salimans, David J Fleet, and Mohammad Norouzi. 2022b. Image super-resolution via iterative refinement. *IEEE Transactions on Pattern Analysis and Machine Intelligence*.

Christoph Schuhmann, Romain Beaumont, Richard Vencu, Cade Gordon, Ross Wightman, Mehdi Cherti, Theo Coombes, Aarush Katta, Clayton Mullis, Mitchell Wortsman, and 1 others. 2022. Laion-5b: An open large-scale dataset for training next generation image-text models. *Advances in Neural Information Processing Systems*, 35:25278–25294.

Christoph Schuhmann, Richard Vencu, Romain Beaumont, Robert Kaczmarczyk, Clayton Mullis, Aarush Katta, Theo Coombes, Jenia Jitsev, and Aran Komatsuzaki. 2021. Laion-400m: Open dataset of clip-filtered 400 million image-text pairs. *arXiv preprint arXiv:2111.02114*.

Jascha Sohl-Dickstein, Eric Weiss, Niru Maheswaranathan, and Surya Ganguli. 2015. Deep unsupervised learning using nonequilibrium thermodynamics. In *International Conference on Machine Learning*, pages 2256–2265. PMLR.

Jiaming Song, Chenlin Meng, and Stefano Ermon. 2020. Denoising diffusion implicit models. *arXiv preprint arXiv:2010.02502*.

Christian Szegedy, Wojciech Zaremba, Ilya Sutskever, Joan Bruna, Dumitru Erhan, Ian J. Goodfellow, and Rob Fergus. 2014. Intriguing properties of neural networks. In *2nd International Conference on Learning Representations(ICLR)*.

Raphael Tang, Akshat Pandey, Zhiying Jiang, Gefei Yang, Karun Kumar, Jimmy Lin, and Ferhan Ture. 2022. What the daam: Interpreting stable diffusion using cross attention. *arXiv preprint arXiv:2210.04885*.

Ilya O Tolstikhin, Bharath K Sriperumbudur, and Bernhard Schölkopf. 2016. Minimax estimation of maximum mean discrepancy with radial kernels. *Advances in Neural Information Processing Systems*, 29.

Andrey Voynov, Kfir Aberman, and Daniel Cohen-Or. 2022. Sketch-guided text-to-image diffusion models. *arXiv preprint arXiv:2211.13752*.

Eric Wallace, Shi Feng, Nikhil Kandpal, Matt Gardner, and Sameer Singh. 2019. Universal adversarial triggers for attacking and analyzing nlp. In *Proceedings of the 2019 Conference on Empirical Methods in Natural Language Processing and the 9th International Joint Conference on Natural Language Processing (EMNLP-IJCNLP)*, pages 2153–2162.

Boxin Wang, Hengzhi Pei, Boyuan Pan, Qian Chen, Shuohang Wang, and Bo Li. 2020. T3: Tree-autoencoder constrained adversarial text generation for targeted attack. In *Proceedings of the 2020 Conference on Empirical Methods in Natural Language Processing (EMNLP)*, pages 6134–6150.

Ruochen Wang, Ting Liu, Cho-Jui Hsieh, and Boqing Gong. 2024. On discrete prompt optimization for diffusion models. In *International Conference on Machine Learning*.

Tengfei Wang, Ting Zhang, Bo Zhang, Hao Ouyang, Dong Chen, Qifeng Chen, and Fang Wen. 2022a. Pretraining is all you need for image-to-image translation. In *arXiv*.

Zijie J. Wang, Evan Montoya, David Munechika, Haoyang Yang, Benjamin Hoover, and Duen Horng Chau. 2022b. DiffusionDB: A large-scale prompt gallery dataset for text-to-image generative models. *arXiv:2210.14896 [cs]*.

Lei Xu, Yangyi Chen, Ganqu Cui, Hongcheng Gao, and Zhiyuan Liu. 2022. Exploring the universal vulnerability of prompt-based learning paradigm. In *Findings of the Association for Computational Linguistics: NAACL 2022*, pages 1799–1810.

Yijun Yang, Ruiyuan Gao, Xiaosen Wang, Nan Xu, and Qiang Xu. 2023. Mma-diffusion: Multimodal attack on diffusion models. *arXiv preprint arXiv:2311.17516*.

Zhuoyi Yang, Jiayan Teng, Wendi Zheng, Ming Ding, Shiyu Huang, Jiazheng Xu, Yuanming Yang, Wenyi Hong, Xiaohan Zhang, Guanyu Feng, and 1 others. 2024. Cogvideox: Text-to-video diffusion models with an expert transformer. *arXiv preprint arXiv:2408.06072*.

Chaoning Zhang, Philipp Benz, Adil Karjauv, Jae Won Cho, Kang Zhang, and In So Kweon. 2022a. Investigating top-k white-box and transferable black-box attack. In *Proceedings of the IEEE/CVF Conference on Computer Vision and Pattern Recognition*, pages 15085–15094.

Chenyu Zhang, Lanjun Wang, and Anan Liu. 2024. Revealing vulnerabilities in stable diffusion via targeted attacks. *arXiv preprint arXiv:2401.08725*.

Jie Zhang, Bo Li, Jianghe Xu, Shuang Wu, Shouhong Ding, Lei Zhang, and Chao Wu. 2022b. Towards efficient data free black-box adversarial attack. In *Proceedings of the IEEE/CVF Conference on Computer Vision and Pattern Recognition (CVPR)*, pages 15115–15125.

Lvmin Zhang and Maneesh Agrawala. 2023. Adding conditional control to text-to-image diffusion models. *arXiv preprint arXiv:2302.05543*.

Wei Emma Zhang, Quan Z Sheng, Ahoud Alhazmi, and Chenliang Li. 2020. Adversarial attacks on deep-learning models in natural language processing: A survey. *ACM Transactions on Intelligent Systems and Technology (TIST)*, 11(3):1–41.

Haomin Zhuang, Yihua Zhang, and Sijia Liu. 2023. A pilot study of query-free adversarial attack against stable diffusion. *arXiv preprint arXiv:2303.16378*.

A Related Work

Diffusion models (DMs) (Sohl-Dickstein et al., 2015; Ho et al., 2020; Song et al., 2020) are a powelful family of generative models that attract great attention recently. In the diffusion process, the data distribution is diffused to an isotropic Gaussian by continually adding Gaussian noises. The reverse process recovers the original input from a Gaussian noise by denoising. DMs have been widely applied to T2I generation. GLIDE (Nichol et al., 2022) first achieves this by integrating the text feature into transformer blocks in the denoising process. Subsequently, increasing effort is devoted to this field to improve the performance of T2I generation, with DALL-E (Ramesh et al., 2021), Cogview (Ding et al., 2021), Make-A-Scene (Gafni et al., 2022), Stable Diffusion (Rombach et al., 2022), Imagen (Saharia et al., 2022a), and Hyper-SD (Ren et al., 2024) as popular examples. A prevalent strategy nowadays is to perform denoising in the feature space while introducing the text condition by cross-attention mechanisms (Tang et al., 2022). However, textual conditions cannot provide the synthesis results with more structural guidance. To remediate this, there are also many other kinds of DMs conditioning on factors beyond text descriptions, such as PITI (Wang et al., 2022a), ControlNet (Zhang and Agrawala, 2023) and Sketch-Guided models (Voynov et al., 2022).

Adversarial attacks typically deceive DNNs by integrating carefully-crafted tiny perturbations into input data (Szegedy et al., 2014; Zhang et al., 2020). Based on how an adversary interacts with the victim model, adversarial attacks can be categorized into white-box attacks (Zhang et al., 2022a; Meng and Wattenhofer, 2020; Xu et al., 2022) (with full access to the victim model) and black-box attacks (Zhang et al., 2022b; He et al., 2021) (with limited access to the victim model). Adversarial attacks on text can also be categorized in terms of the level of granularity of the perturbations. Character-level attacks (Eger et al., 2019b; Formento et al., 2023) modify individual characters in words to force the tokenizer to process multiple unrelated embeddings instead of the original, resulting in decreased performance. Word-level attacks (Li et al., 2021; Lee et al., 2022) employ a search algorithm to locate useful perturbing embeddings or operations that are clustered close to the candidate attack word's embedding given a similarity constraint (e.g., the Universal Sentence Encoder (Cer et al., 2018)).

Rule	Ori. Sentence	Adv. Sentence
Typo	A red ball on green grass under a blue sky.	A rde ball on green grass under a blue skky.
Glyph	A red ball on green grass under a blue sky.	A rêd ball 0n green grass under a blue sky.
Phonetic	A red ball on green grass under a blue sky.	A read ball on green grass under a blue SKY.

Table 3: Examples of our perturbation rules.

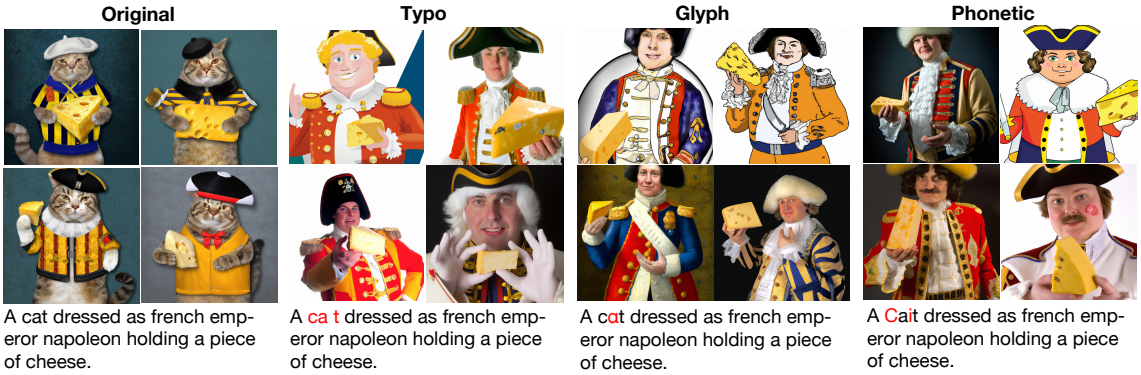

Figure 6: An illustration of adversarial attack against DALL-E 2 with **MMD** attack objective.

Sentence-level attacks (Wang et al., 2020; Han et al., 2020) refer to making changes to sentence structures in order to prevent the model from correctly predicting the outcome. Multi-level attacks (Gupta et al., 2021; Wallace et al., 2019) combine multiple types of perturbations, making the attack cumulative. Recent studies (Millière, 2022; Maus et al., 2023; Zhuang et al., 2023; Yang et al., 2023; Zhang et al., 2024; Wang et al., 2024) have explored the over-sensitivity of T2I DMs to prompt perturbations in the text domain with malicious word synthesis, phrase synthesis, visual substitution and adding distraction. (Zhuang et al., 2023) also reveal the vulnerability of T2I models and attributes it to the weak robustness of the used text encoders.

B Examples of Perturbation Rules

We present concrete examples of the three perturbation rules used in our attack (Typo, Glyph, and Phonetic) in Table 3.

C Proof of Eq. (3)

$$\begin{aligned}\mathcal{D}_{\mathrm{KL}}(p_\theta(x|c')\|p_\theta(x|c)) &\approx \mathcal{D}_{\mathrm{KL}}(p_\theta(x|c')\|p_\phi(x|c)) \\ &= \mathbb{E}_{p_\theta(x|c')}\left[\log \frac{p_\theta(x|c')}{p_\phi(x|c)p(c)} + \log p(c)\right] \\ &= \mathbb{E}_{p_\theta(x|c')}[-e_\phi(x,c)] + \mathbb{E}_{p_\theta(x|c')}[\log p_\theta(x|c')] + C\end{aligned} \tag{11}$$

D Human Evaluation Details

Three human evaluators are employed to evaluate the consistency between the image and text. Let N_1 represent the number of images generated by the original text that are consistent with the original text, and N_2 represent the number of images generated by the adversarial text that are consistent with original text. If $(N_2 - N_1) > 1$, the attack on that particular prompt text is deemed meaningless. Let's assume the frequency of samples where $(N_2 - N_1) > 1$ as N_u, and the frequency of successful attack, $(N_1 - N_2 > 1)$, as N_c. The score (Hum.Eval) for all three evaluators is given by:

$$\begin{aligned}S_{\text{Hum.Eval}} &= \frac{1}{3}\sum_{i=1}^{3}\left(\frac{N_c^{(i)}}{N_{\text{total}} - N_u^{(i)}}\right) \\ &= \frac{1}{3}\sum_{i=1}^{3}\left(\frac{\sum_{i=1}^{N_{\text{total}}}\mathbf{1}\left(N_1^{(i)} - N_2^{(i)} > 1\right)}{N_{\text{total}} - \sum_{i=1}^{N_{\text{total}}}\mathbf{1}\left(N_2^{(i)} - N_1^{(i)} > 1\right)}\right)\end{aligned} \tag{12}$$

E Experiment Result

E.1 Real-world Attack on SDXL

To further explore how model robustness relates to model size, we also conduct real-world attack experiment on **SDXL** (Podell et al., 2023), a 2.6B SD model, with the same setting of attack experiment on SD v2.1 and 2ST attack objective. Table 4 demonstrates that SDXL exhibits superior robustness compared to SD v2.1. We present some cases of both SD v2.1 and SDXL in Figure 9. Additionally, Figure 8 in shows several adversarial cases where SDXL remains unaffected while SD v2.1 is attacked successfully.

Panda mad scientist mixing sparkling chemicals, artstation. | Pan da mad scientist mixing sparkling chemicals, artstation. | Ṕanda mad scientist mixing sparkling chemicals,artstation. | Painda mad scientist mixing sparkling chemicals, artstation.

Figure 7: An illustration of adversarial attack against DALL-E 2 with **2ST** attack objective.

Dataset	Attacker	Ori. S_{I2T}	Ave. Len.	L-distance	Adv. S_{I2T}	Ave. Query	Hum. Eval.
ChatGPT-GP	Typo	29.23±1.95	10.41	3.04	24.16±3.32	20.59	79.36%
	Glyph			2.47	24.19±3.01	19.84	80.25%
	Phonetic			5.45	23.15±3.84	18.18	82.89%
DiffusionDB	Typo	30.47±2.48	10.62	2.33	23.67±3.59	17.82	73.44%
	Glyph			1.95	23.21±3.43	17.01	72.19%
	Phonetic			5.18	22.99±3.54	17.17	73.18%
LAION-COCO	Typo	29.65±2.14	9.17	2.21	22.24±3.76	15.33	78.32%
	Glyph			1.94	22.22±3.71	16.12	79.05%
	Phonetic			5.17	22.39±3.92	16.75	78.11%
SBU Corpus	Typo	26.52±3.13	11.69	3.11	21.23±3.72	22.41	81.64%
	Glyph			2.58	20.16±3.93	20.92	82.29%
	Phonetic			5.97	19.98±4.05	20.32	83.16%

Table 4: Real-world attack with the **2ST** attack objective on SDXL.

E.2 More Cases on SD v2.1 and SDXL

As a supplement to the experiments on SD and SDXL in Section 4, we present two additional cases for each of the models, shown in Figure 9.

E.3 Case Study on DALL-E 2

DALL-E 2 (Ramesh et al., 2022) is also a powerful image generation model that can create realistic and diverse images from textual descriptions. We then conduct a case study with the same attack method used in Stable Diffusion before. The results respectively obtained with the attack objective MMD and 2ST are presented in Figure 6 and Figure 7. As a supplement to the case study experiments on DALL-E 2, we also present two additional cases for each of the optimization objectives, MMD and 2ST, shown in Figure 10.

E.4 Evaluation on the Defense Side

We used two widely used correctors, LanguageTool[1] and Online Correction[2] as the corrector. Then we selected 100 successfully attacked text samples for each perturbation rule with 2ST attack objective from the ChatGPT-GP dataset, following before settings. Finally, we evaluated the samples modified by these typo-correctors to determine whether they were successfully repaired. Note that if the corrector provided more than one recommended correct word, we utilized the first recommended word. Table 5 presents the comparison on **Successful Repair Rate (SRR)**.

Typo Corrector	Perturbation Rule	SRR
LanguageTool	Typo	68%
	Glyph	39%
	Phonetic	21%
Online Correction	Typo	81%
	Glyph	42%
	Phonetic	25%

Table 5: Successful Repair Rate (SRR) of two auto-correctors to 3 perturbation rules.

It is shown that auto-typo correctors can partially correct human mistakes from typo perturbations in our work. However, correcting a little fiercely perturbed sentence caused by glyphs and phonetics

[1] https://languagetool.org/
[2] https://www.onlinecorrection.com/

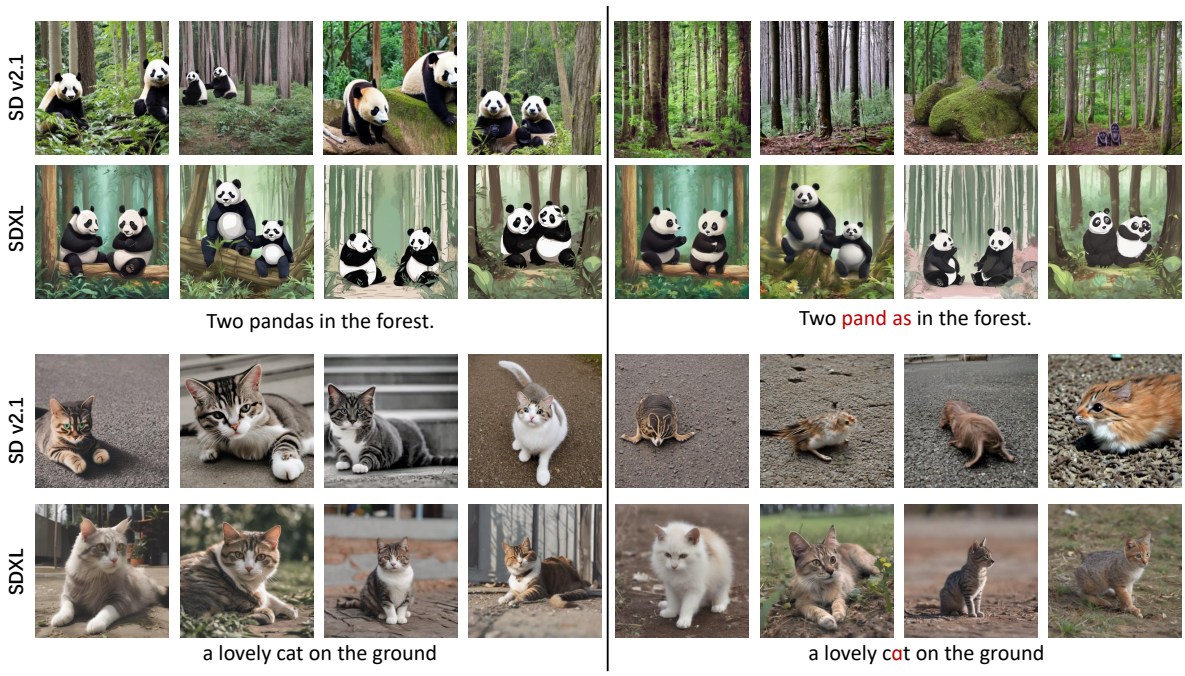

Figure 8: Adversarial cases where SDXL remains unaffected while SD v2.1 is attacked successfully.

Dataset	Attacker	Ori. S_{I2T}	Ave. Len.	L-distance	Adv. S_{I2T}	Ave. Query	Hum. Eval.
ChatGPT-GP	Typo	27.61±2.07	10.41	2.65	24.61±3.32	16.97	79.36%
	Glyph			2.09	24.94±3.01	16.86	77.45%
	Phonetic			5.13	26.67±3.74	15.71	78.68%

Table 7: Real-world attack with the **DI** attack objective.

proves challenging. Hence, our method can remain effective against auto-typo correctors. It is also worth noting that these correctors often struggle to automatically rectify words in a manner that aligns with the user's intent when human intervention is not involved in the word selection process from the correction word list.

E.5 Real-word Attack With DI Attack Objective

We conduct a real-world attack with the DI attack objective(i.e. single-image guidance attack) on the ChatGPT-GP dataset, employing the same settings as the other objectives detailed in Section 4. Table 7 illustrates that the $Adv.S_{I2T}$ and human evaluation scores associated with this objective are relatively low. This observation suggests that the attack with the DI objective may be susceptible to overfitting on a single image.

E.6 Human Evaluation for Adversarial Text

To prove that human evaluation won't be affected by the adversarial noise of text. We conduct the experiment to evaluate the difference between the image content and the actual meaning of the adversarial text. We let N_1 represent the number of images generated by the original text that are consistent with the original text as original, while N_2 represents the number of images generated by the adversarial text that are consistent with the **adversarial text**. The new overall human evaluation score is calculated in the same way as before. Table 9 shows the new overall human evaluation on the same adversarial dataset generated under real-world attack with the 2ST attack objective in section 4. We found that although the new overall human evaluation score will decrease to some extent compared to the old score, the change is not significant, indicating that human evaluations are not affected by the adversarial text.

E.7 Lexical Properties of the Modified Word

The modified words of adversarial text can be nouns, adjectives and verbs. In descriptive text about objects, there is a greater occurrence of modified words in nouns. It is important to note that our approach aims to identify words that are most important for the model, rather than those deemed

(a) SD v2.1: Case 1

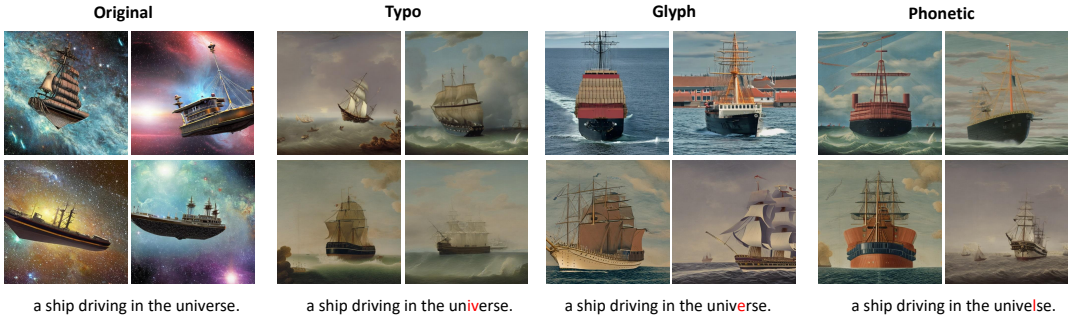

(b) SD v2.1: Case 2

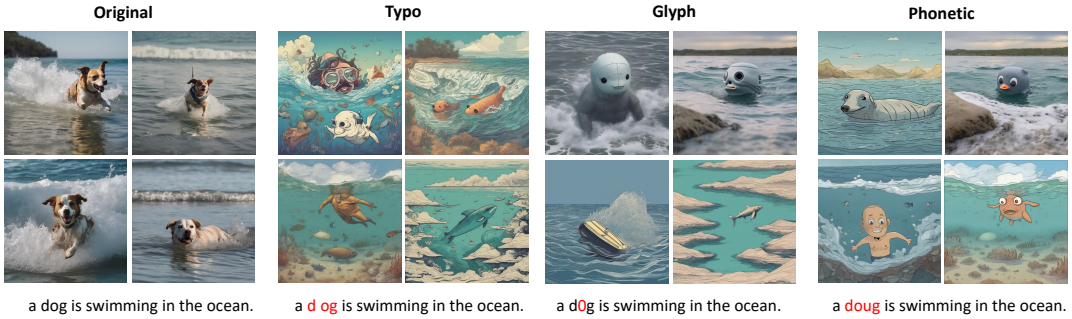

(c) SDXL: Case 1

(d) SDXL: Case 2

Figure 9: More illustration cases of adversarial attack against SD v2.1 and SDXL with 2ST attack objective. Each of these models has two cases.

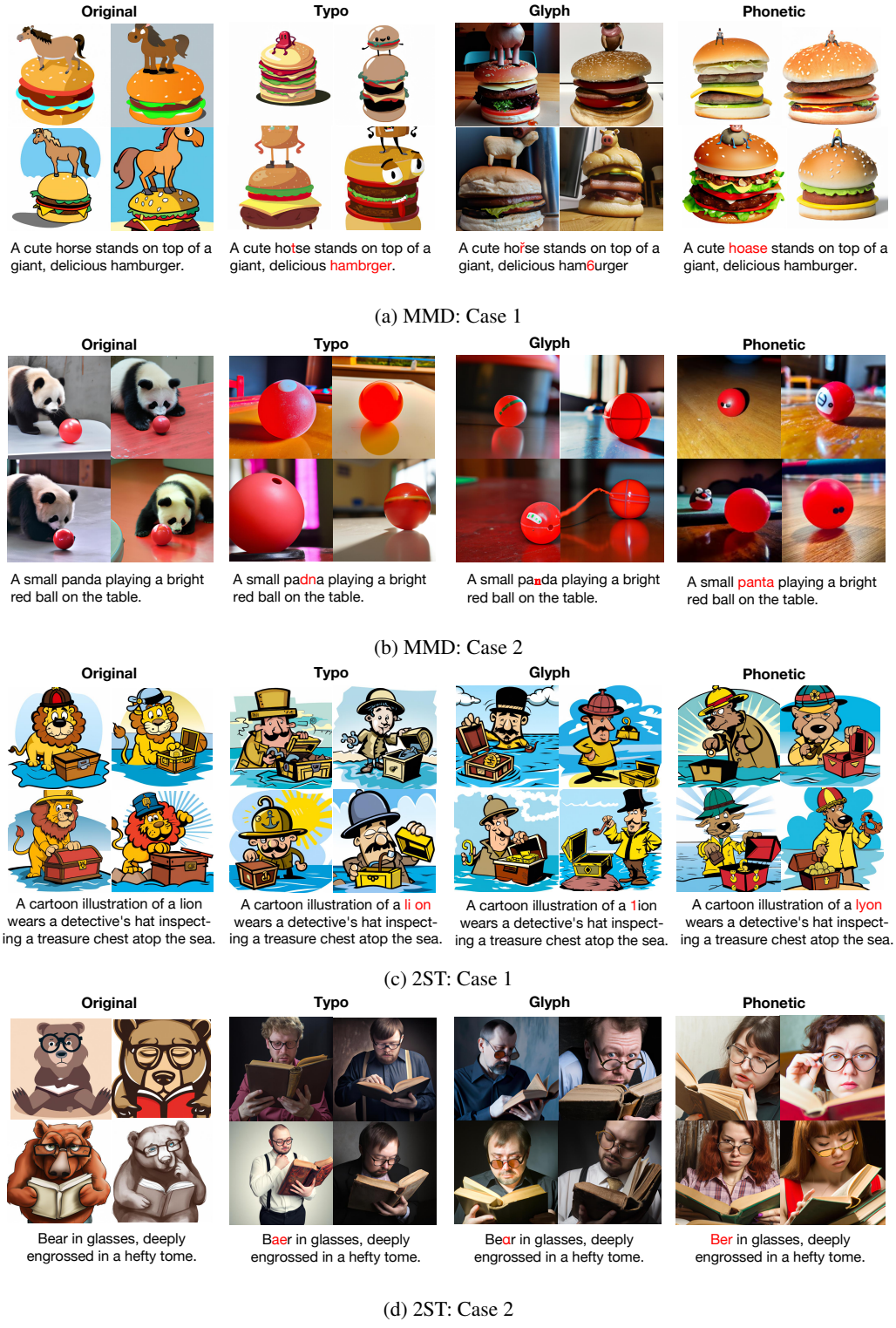

Figure 10: Illustrations of adversarial attack against DALL-E 2 with MMD or 2ST attack objective. Each objective has two cases.

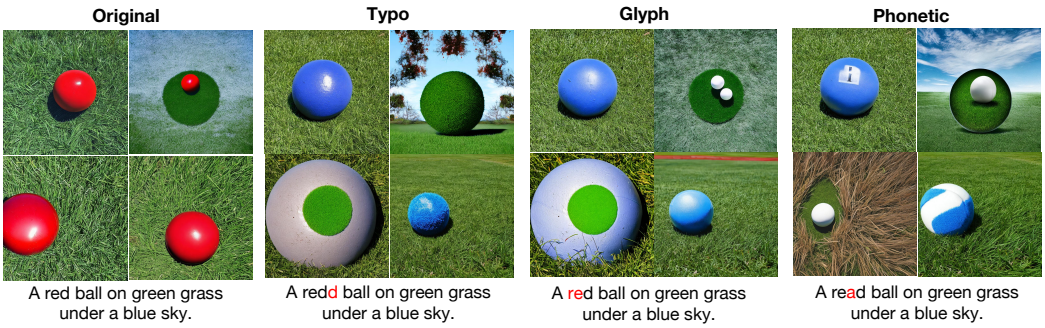

(a) Case with modified adjectives.

(b) Case with modified verbs.

Figure 11: Cases without noun modification.

most important by humans. Therefore, in theory, it is not limited to a specific part of speech. Figure 11 shows some cases without noun modification.

F Discussion on Human Attack and Word-level Attack

F.1 Human Attack

Firstly, we would like to emphasize the effectiveness of our adversarial optimization algorithm. In order to demonstrate this, we compare our method with human attack without algorithmic interventions. We randomly selected a set of sentences and made random modifications to the most important words based on human intuition. Remarkably, we observed that a lot of sentences with these modifications did not result in DMs generating incorrect images. This further substantiates the effectiveness of our attack algorithm. We present two illustrative cases in Figure 12. The results emphasize the difficulty of this attack task and show the effectiveness of our method.

F.2 Word-level Attack

Then we talk about the other level attacks such as word-level attacks. Due to the high sensitivity of the DM to individual words in the prompt, word-level attacks such as synonym replacement or context filling were not employed in this study. If we were to use synonym replacements and substitute words with less commonly used ones, those words themselves might have multiple meanings. In such cases, the model is likely to generate images based on alternative meanings, making the substituted words different in the context of the sentence, even though they may be synonyms in terms of individual words. Therefore, a more stringent restriction is required for word-level replacements. It is precisely because of this reason that traditional text-based attack methods are not applicable to image-text generation. For instance, in sentiment classification tasks, they only consider the overall sentiment of the entire sentence, and the ambiguity of a particular word does not significantly impact the overall result. However, this sensitivity becomes crucial in the context of T2I. Hence, further research is needed to explore word-level and sentence-level attacks on T2I generation models.

To better illustrate our point, we conducted a comparison on the semantic consistency between word-level attack and our method. We chose two classical textual word-level adversarial attack

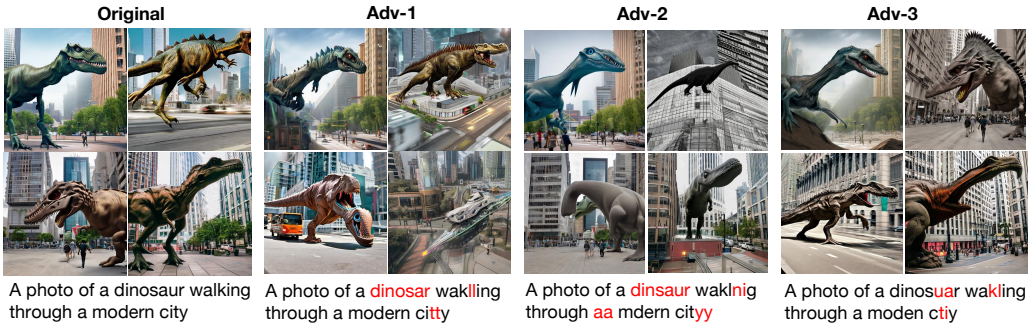

(a) Case 1

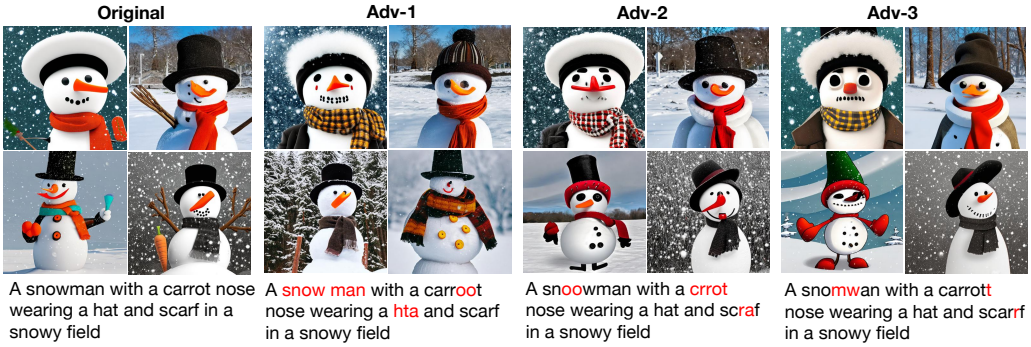

(b) Case 2

Figure 12: Illustrations of human attack method against Stable Diffusion. Adversarially modified content is highlighted in red.

Attack Method	Perturbation Level	DCR
BERTAttack	Word-level	19%
PWWS	Word-level	24%
Our Method(Typo)	Char-level	82%
Our Method(Glyph)	Char-level	96%
Our Method(Phonetic)	Char-level	73%

Table 8: Comparison on DCR between word-level attacks and our method.

Dataset	Attacker	Hum. Eval.	Hum. Eval. (New)
ChatGPT-GP	Typo	84.34%	82.19%
	Glyph	84.65%	83.42%
	Phonetic	86.16%	82.06%
DiffusionDB	Typo	76.64%	74.34%
	Glyph	76.64%	75.26%
	Phonetic	75.51%	73.61%
LAION-COCO	Typo	80.21%	78.28%
	Glyph	81.89%	80.94%
	Phonetic	79.32%	77.02%
SBU Corpus	Typo	84.34%	82.13%
	Glyph	85.41%	85.57%
	Phonetic	85.41%	81.95%

Table 9: Exploring whether human evaluation will be affected by the adversarial noise of text on real-world attack with the **2ST** attack objective.

algorithms in natural language processing(NLP), BERTAttack (Li et al., 2020) and PWWS (Ren et al., 2019) to compare with our method with 3 perturbation rules (typo, glyph and phonetic) with same optimization objective. We sampled 100 texts from successfully attacked texts for each attack method and evaluated the description consistency between these adversarial texts and their corresponding original texts by humans. To avoid bias, we evaluated each text with three people and took the plural of the three people's opinions as the final decision. Table 8 below presents the comparison on **Description Consistency Rate (DCR)** and shows that our method based on character level perturbation can keep the description consistency far more than word-level attack methods such as BERTAttack and PWWS.

We also list some examples generated by word-level adversarial attack methods in Table 10. It is evident that significant semantic changes have occurred in the examples presented. Therefore, word-level attacks in still have a long way to go in T2I adversarial attack.

G LLM Usage

We used an OpenAI LLM (GPT-5) as a writing and formatting assistant. In particular, it helped

Attack Method	Ori. Text	Adv. Text
BERTAttack	A red ball on green grass under a blue sky.	A red field on green grass under a blue sky.
	A white cat sleeping on a windowsill with a flower pot nearby.	A green cat sleeping on a windowsill with a flower pot nearby.
	A wooden chair sitting in the sand at a beach.	A wooden camera sitting in the sand at a beach.
PWWS	A red ball on green grass under a blue sky.	A red orchis on green grass under a blue sky
	A white cat sleeping on a windowsill with a flower pot nearby.	A white guy sleeping on a windowsill with a flower pot nearby
	A wooden chair sitting in the sand at a beach.	A wooden chairwoman sitting in the baroness at a beach.

Table 10: Word-level attack examples by BERTAttack and PWWS with **2ST** attack objective.

refine grammar and phrasing, improve clarity, and suggest edits to figure/table captions and layout (e.g., column alignment, caption length, placement). The LLM did not contribute to research ideation, experimental design, implementation, data analysis, or technical content beyond surface-level edits. All outputs were reviewed and edited by the authors, who take full responsibility for the final text and visuals.